Electronic Supplementary Material (ESI) for Dalton Transactions.

Design of Dual-switch Fluorescence Intensity Ratio Thermometry with High Sensitivity and Thermochromism Based on Combination Strategy of Intervalence Charge Transfer and Up-conversion Fluorescence Thermal Enhancement

Qiang Wang[a,b], Min Liao[a,b], Qiuming Lin[a,b], Mingxiang Xiong[a,b], Xin Zhang[c], Huafeng Dong[c], Zhiping Lin[c], Minru Wen[c], Daoyun Zhu[b], Zhongfei Mu[b,], Fugen Wu[a,*]*

[a] School of Materials and Energy, Guangdong University of Technology, Waihuan Xi Road, No.100, Guangzhou, 510006, PR China

[b] Experimental Teaching Department, Guangdong University of Technology, Waihuan Xi Road, No.100, Guangzhou, 510006, PR China

[c] School of Physics & Optoelectronic Engineering, Guangdong University of Technology, Waihuan Xi Road, No.100, Guangzhou, 510006, PR China

*corresponding author: muzhongfei@gdut.edu.cn; wufg@gdut.edu.cn

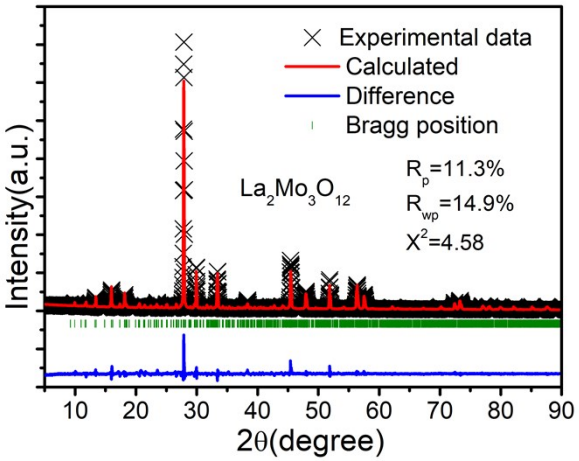

Fig. S1. Results of XRD pattern Rietveld refinement of synthesized $La_2Mo_3O_{12}$ (Experimental (crosses) and calculated (red solid line), the blue solid line represents the difference between experimental and calculated data and the green sticks mark the Bragg reflection positions).

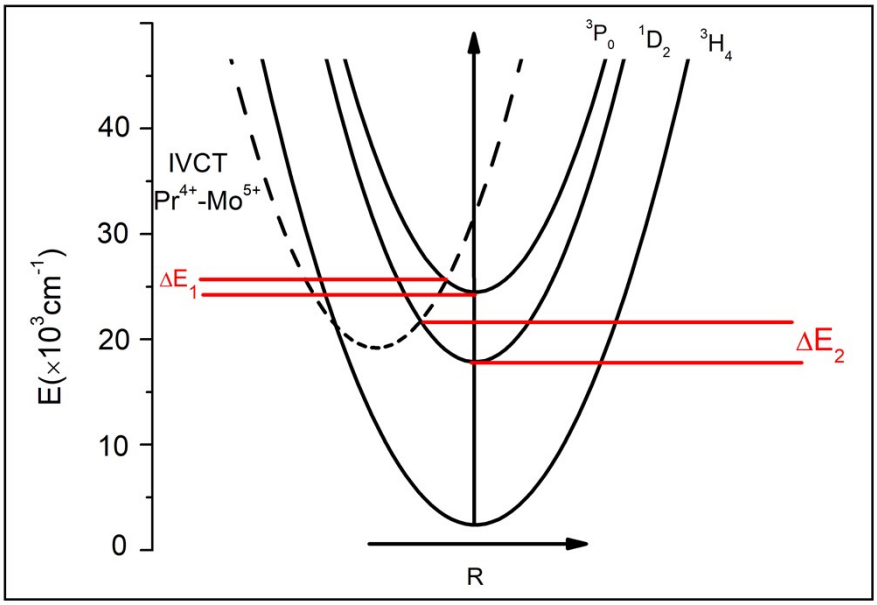

Fig. S2. Schematic configurational coordinate diagram for Pr^{3+} in the $La_2Mo_3O_{12}$.

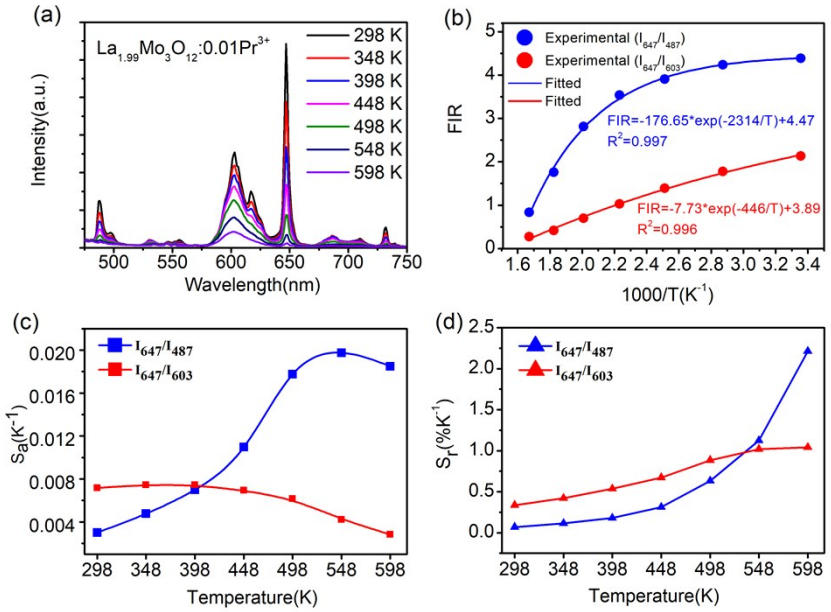

Fig. S3. (a) Temperature dependent PL spectra of the $La_{1.99}Mo_3O_{12}$:0.01Pr^{3+} sample (b) Experimental and fitted plots of FIR (I_{647}/I_{487} and I_{647}/I_{603}) versus 1000/T. (c) The calculated plots of S_a and versus T. (d) The calculated plots of S_r and versus T.

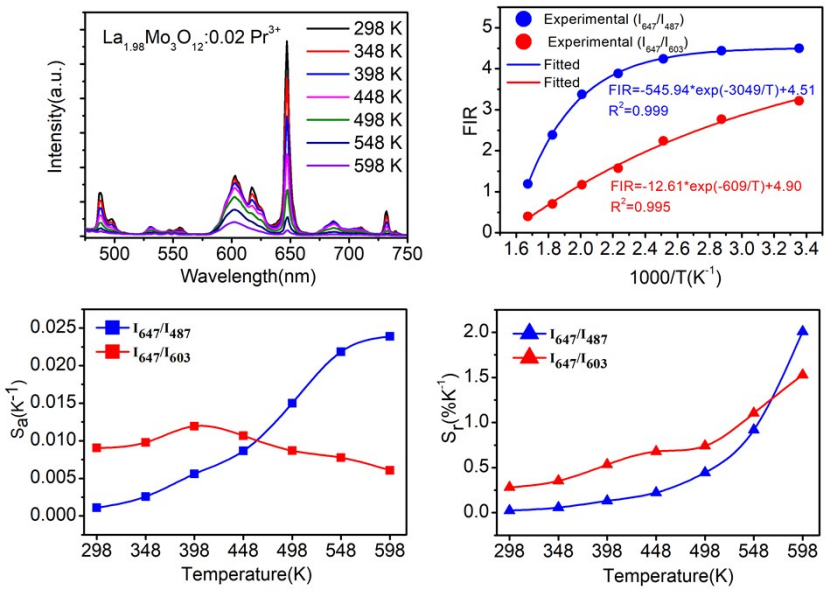

Fig. S4 (a) Temperature dependent PL spectra of the $La_{1.98}Mo_3O_{12}$: $0.02Pr^{3+}$ sample (b) Experimental and fitted plots of FIR (I_{647}/I_{487} and I_{647}/I_{603}) versus 1000/T. (c) The calculated plots of S_a and versus T. (d) The calculated plots of S_r and versus T.

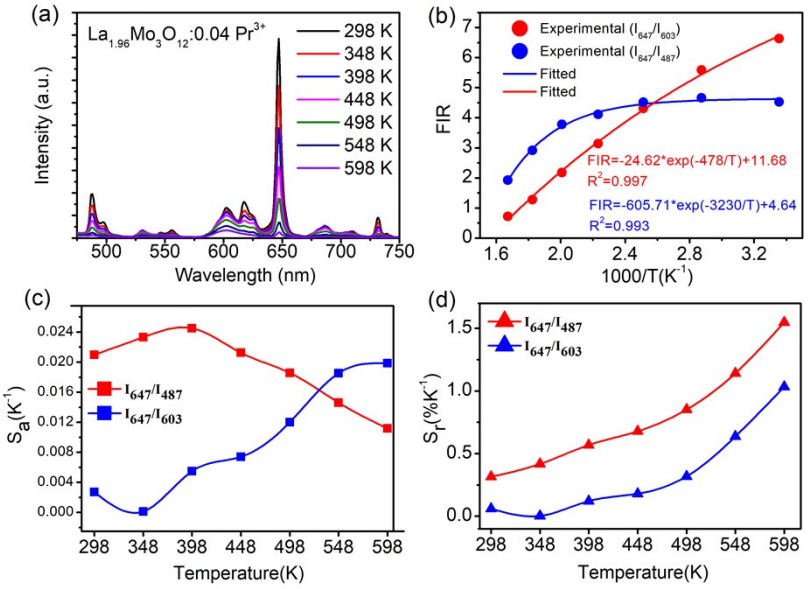

Fig. S5 (a) Temperature dependent PL spectra of the $La_{1.96}Mo_3O_{12}$:$0.04Pr^{3+}$ sample (b) Experimental and fitted plots of FIR (I_{647}/I_{487} and I_{647}/I_{603}) versus 1000/T. (c) The calculated plots of S_a and versus T. (d) The calculated plots of S_r and versus T.

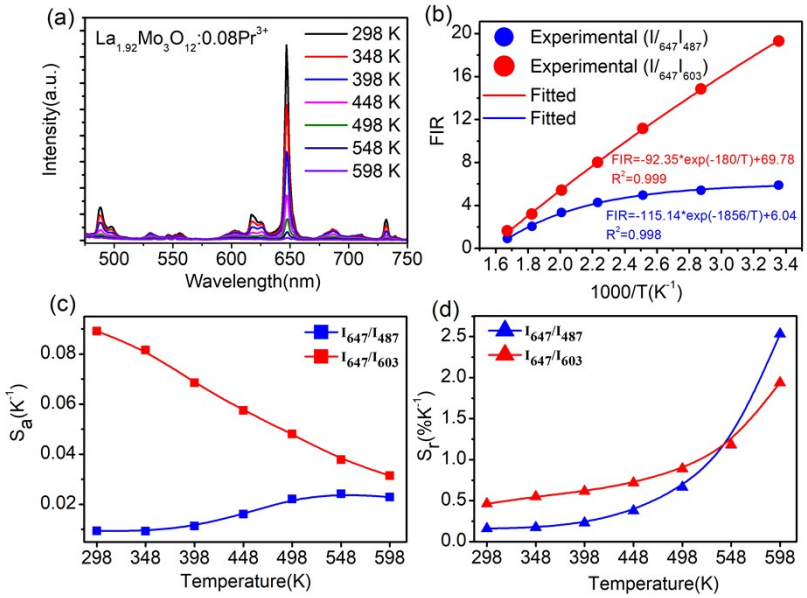

Fig. S6 (a) Temperature dependent PL spectra of the $La_{1.92}Mo_3O_{12}$:0.08Pr^{3+} sample (b) Experimental and fitted plots of FIR (I_{647}/I_{487} and I_{647}/I_{603}) versus 1000/T. (c) The calculated plots of S_a and versus T. (d) The calculated plots of S_r and versus T.

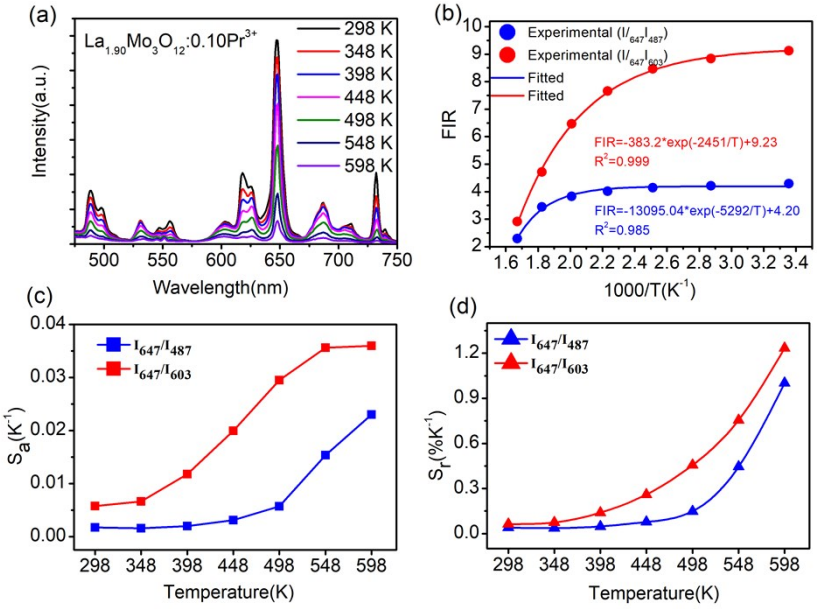

Fig. S7 (a) Temperature dependent PL spectra of the $La_{1.90}Mo_3O_{12}$:0.10Pr^{3+} sample (b) Experimental and fitted plots of FIR (I_{647}/I_{487} and I_{647}/I_{603}) versus 1000/T. (c) The calculated plots of S_a and versus T. (d) The calculated plots of S_r and versus T.

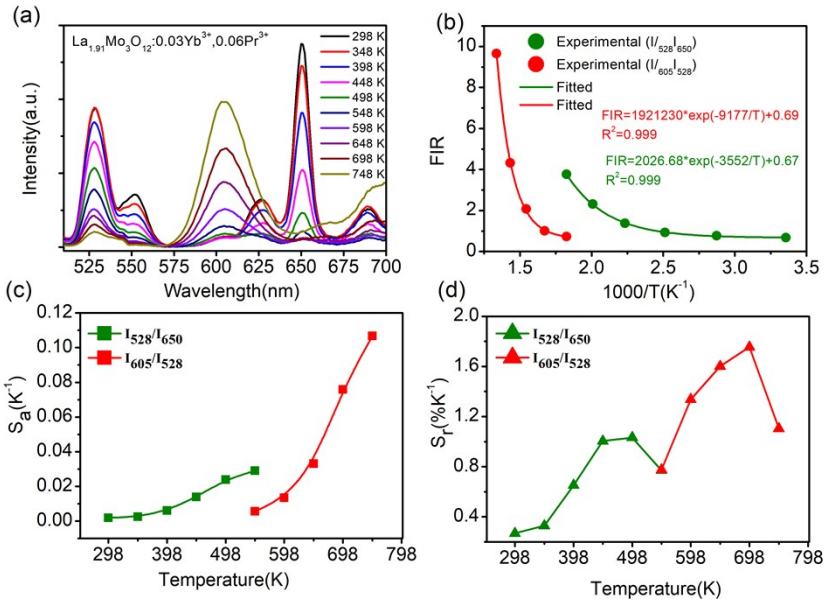

Fig. S8 (a) Temperature dependent PL spectra of the $La_{1.91}Mo_3O_{12}$:0.03 Yb^{3+}, 0.06Pr^{3+} sample (b) Experimental and fitted plots of two stage FIR (I_{528}/I_{650} and I_{605}/I_{650}) from 298 to 748 K versus 1000/T. (c) The calculated plots of S_a and versus T. (d) The calculated plots of S_r and versus T.

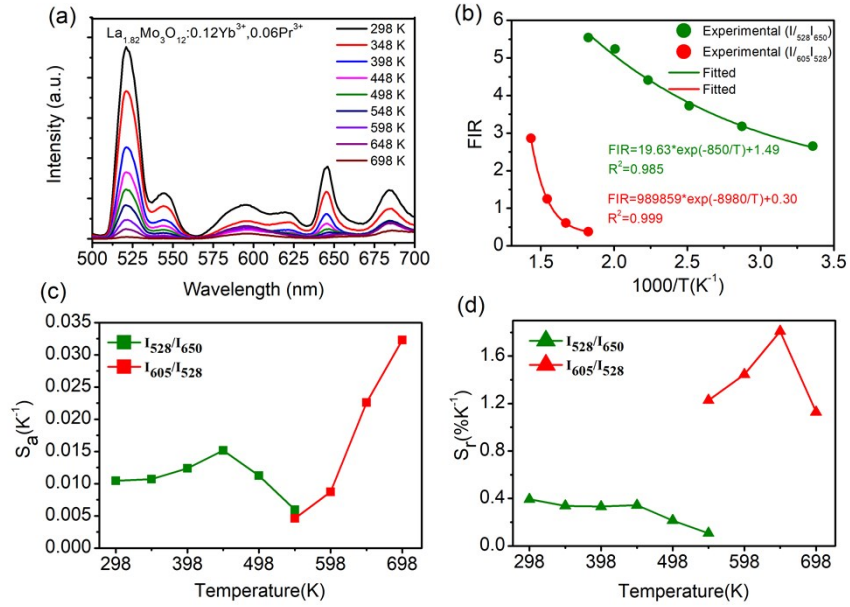

Fig. S9 (a) Temperature dependent PL spectra of the $La_{1.82}Mo_3O_{12}$:0.12 Yb^{3+}, 0.06Pr^{3+} sample (b) Experimental and fitted plots of two stage FIR (I_{528}/I_{650} and I_{605}/I_{650}) from 298 to 698 K versus 1000/T. (c) The calculated plots of S_a and versus T. (d) The calculated plots of S_r and versus T.

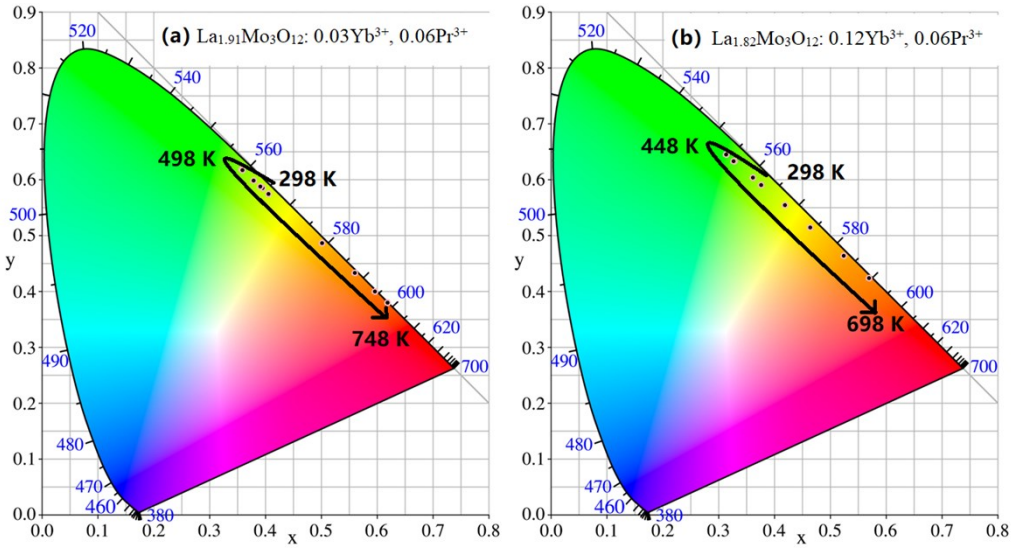

Fig. S10 CIE chromaticity diagram of (a) $La_{1.91}Mo_3O_{12}$: $0.03Yb^{3+}$, $0.06Pr^{3+}$ materials; (b) $La_{1.82}Mo_3O_{12}$: $0.12Yb^{3+}$, $0.06Pr^{3+}$ materials.

Table S1 Temperature sensing performances of Pr^{3+} single-activated $La_2Mo_3O_{12}$ materials based on PL spectra excited by 450 nm ($^3P_0 \rightarrow {}^3H_4$, $^1D_2 \rightarrow {}^3H_4$ and $^3P_0 \rightarrow {}^3F_2$ transitions).

Samples	$S_{a\text{-}max}$ (K^{-1})	$S_{r\text{-}max}$(%K^{-1})	Temperature range (K)
$La_{1.99}Mo_3O_{12}$:$0.01Pr^{3+}$	0.020 (598 K)	2.213 (598 K)	298-598
$La_{1.98}Mo_3O_{12}$:$0.02Pr^{3+}$	0.024 (598 K)	2.008 (598 K)	298-598
$La_{1.96}Mo_3O_{12}$:$0.04Pr^{3+}$	0.025 (398 K)	1.548 (598 K)	298-598
$La_{1.94}Mo_3O_{12}$:$0.06Pr^{3+}$	0.060 (298 K)	2.172 (598 K)	298-598
$La_{1.92}Mo_3O_{12}$:$0.08Pr^{3+}$	0.089 (298 K)	2.532 (598 K)	298-598
$La_{1.90}Mo_3O_{12}$:$0.10Pr^{3+}$	0.036 (598 K)	1.234 (598 K)	298-598

Table S2 Temperature sensing performances of Yb^{3+}, Pr^{3+} co-activated $La_2Mo_3O_{12}$ materials based on PL spectra excited by 980 nm ($^3P_1 \rightarrow {}^3H_5$, $^1D_2 \rightarrow {}^3H_4$ and $^3P_0 \rightarrow {}^3F_2$ transitions).

Samples	$S_{a\text{-}max}$ (K^{-1})	$S_{r\text{-}max}$(%K^{-1})	Temperature range (K)
$La_{1.91}Mo_3O_{12}$:0.03 Yb^{3+}, 0.06Pr^{3+}	0.111 (748 K)	1.754 (698 K)	298-748

$La_{1.88}Mo_3O_{12}$:0.06 Yb^{3+}, 0.06Pr^{3+}	0.026 (648 K)	4.325 (598 K)	298-748
$La_{1.82}Mo_3O_{12}$:0.12 Yb^{3+}, 0.06Pr^{3+}	0.032 (698 K)	1.809 (648 K)	298-698

Table S3 CIE coordinates of Yb^{3+}, Pr^{3+} co-activated $La_2Mo_3O_{12}$ materials excited by 980 nm.

Samples	Temperature (K)	*x′*	*y′*
$La_{1.91}Mo_3O_{12}$: 0.03 Yb^{3+}, 0.06Pr^{3+}	298	0.3950	0.5848
	348	0.3910	0.5879
	398	0.3792	0.5984
	448	0.3569	0.6186
	498	0.3585	0.6173
	548	0.4054	0.5744
	598	0.5018	0.4861
	648	0.5596	0.4332
	698	0.5961	0.3999
	748	0.6187	0.3797
$La_{1.88}Mo_3O_{12}$: 0.06 Yb^{3+}, 0.06Pr^{3+}	298	0.3797	0.5969
	348	0.3792	0.5970
	398	0.3711	0.6038
	448	0.3565	0.6165
	498	0.3333	0.6368
	548	0.3319	0.6375
	598	0.3916	0.5847
	648	0.4985	0.4873
	698	0.5786	0.4156
	748	0.6130	0.3849
$La_{1.82}Mo_3O_{12}$: 0.12 Yb^{3+}, 0.06Pr^{3+}	298	0.3617	0.6038
	348	0.3275	0.6330
	398	0.3133	0.6454
	448	0.3266	0.6338
	498	0.3764	0.5909
	548	0.4182	0.5550
	598	0.4642	0.5152
	648	0.5240	0.4639
	698	0.5698	0.4240